ACS Partner Journal

ENVIRONMENT & HEALTH

Open Access

pubs.acs.org/EnvHealth

Article

Incomplete versus Sustained Innate-Immune Responses in the Medicinal Leech following Chronic, Environmentally Relevant Per- and Polyfluoroalkyl Substance Exposure

Published as part of Environment & Health special issue "New Pollutants: Challenges and Prospects".

Nicolò Baranzini,[‡] Antonio Calisi,[‡] Gaia Marcolli, Camilla Bon, Davide Rotondo, Davide Gualandris, Laura Pulze, Annalisa Grimaldi,* and Francesco Dondero

Cite This: https://doi.org/10.1021/envhealth.5c00268

Read Online

ACCESS | Metrics & More | Article Recommendations

ABSTRACT: Per- and polyfluoroalkyl substances (PFAS) persist in aquatic systems, yet hazard evaluations still rely largely on short-term tests. We chronically exposed the medicinal leech *Hirudo verbana* for two months to four PFAS congeners at 1 nmol L^{-1} aligned with the EU Drinking Water Directive thresholds (PFAS total = 0.50 μg L^{-1}): a legacy long-chain acid (PFOA), two short-chain ether replacements (HFPO-DA and PFMoBa), and an intermediate methoxy analogue (PFMOPrA). Histology, enzymatic histochemical staining, immunofluorescence, and quantitative polymerase chain reaction tracked the canonical inflammatory sequence, represented by $CD11b^+$ granulocyte influx, $CD31^+$ neovessel formation, and recruitment of $CD45^+/ACP^+$ macrophage-like cells, together with transcriptional responses of oxidative stress genes (*SOD* and *GST*) and two immune mediators (*Hv*RNASET2 and *Hm*AIF-1), chosen for their known role in leech innate immunity. PFOA and PFMOPrA sustained the full CD11b/CD45/CD31 cascade, maintained high ACP activity, and strongly upregulated *Hv*RNASET2, *Hm*AIF-1, *SOD* and *GST*, signaling stability, and tissue-remodeling inflammation. By contrast, HFPO-DA and PFMoBa induced a granulocyte influx but failed to promote macrophage recruitment or neovascularization; *Hv*RNASET2 transcripts rose, whereas *Hm*AIF-1 expression, ACP activity, and CD31 signal remained at the baseline. These outcomes suggest that while all PFAS trigger the same innate-immune program, only PFOA and PFMOPrA sustained its full development. Taken together, these observations suggest that multiple structural and bioactivity determinants, potentially including but not limited to the chain length, shape the sustained response at the chronic level in leeches. This supports the need for multitemporal, policy-relevant PFAS hazard assessment.

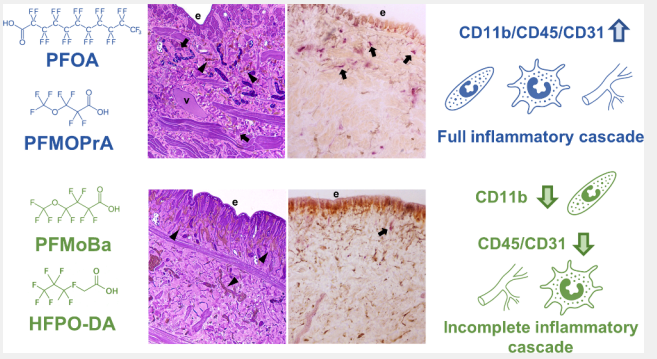

KEYWORDS: *perfluoroalkyl substances, aquatic ecosystem, medicinal leech, inflammation, oxidative stress*

1. INTRODUCTION

Per- and polyfluoroalkyl substances (PFAS) are under intense regulatory and scientific scrutiny owing to their extreme persistence, global ubiquity, and emerging links to immunotoxicity, cancer, and metabolic disease. Legacy long-chain compounds such as perfluorooctanoic acid (PFOA), which represents a long-chain PFCA with well-documented occurrence and persistence, and perfluorooctanesulfonic acid (PFOS) have been detected in human serum worldwide,[1−3] prompting international measures from production phase-outs[4] and the substitution of legacy congeners with shorter chains or ether linkages.[5−11] Recent policy actions span both sides of the Atlantic, including U.S. aquatic-life criteria,[12] EU drinking water group limits,[13] and newly enforceable U.S. drinking water standards,[9] together signaling a broad regulatory shift toward stricter PFAS control in water. Although these measures have reduced environmental emissions of legacy PFAS,[14] they also raise new questions about residual hazards and risks.[15−18] Indeed, it has been also proven that despite their classification, all the most commercially produced PFAS have been detected in many different biological matrices, from soil to waters, and exhibit high rates of bioaccumulation.[19]

Received: July 5, 2025
Revised: November 17, 2025
Accepted: December 4, 2025

The multitude of applications and the advantageous physical properties, such as longevity and high heat stability, make PFAS extremely attractive in terms of applicability, but simultaneously increase the risk associated with their potential dispersion and ecological persistence.[20] Thus, released both from industrial raw materials and directly from consumer products and everyday retail articles, PFAS are able to persist for decades and, regardless of their molecular structure, exhibit prolonged half-life and significant environmental mobility, which confer high bioaccumulative potential and are associated with adverse effects on living organisms.[21,22] Concerning aquatic ecosystems, short-chain PFAS are highly water-soluble and can enrich at the air−water interface, whereas longer-chain congeners exhibit stronger sorption to sediments and greater bioaccumulation potential; these behaviors scale with chain length and headgroup chemistry.[21−24] Across drinking water source waters, national monitoring indicates total PFAS means of ∼90 ng L^{-1} in surface waters and ∼210 ng L^{-1} in groundwater, with hotspot maxima reported up to 7000 ng L^{-1} for PFOS; PFECAs such as HFPO-DA (GenX) have been measured at ∼631 ng L^{-1} at community intakes.[25] Globally, surface and groundwaters typically fall in the single-digit to few-tens of ng L^{-1} range, but industrial/AFFF-impacted sites intermittently reach 10^2−10^3 ng L^{-1} and, in some cases, μg L^{-1}.[26] Unfortunately, one of the primary routes by which organisms come into contact with PFAS is the intake of contaminated water. Groundwater, in particular, serves as a crucial source for drinking water, providing a significant portion of the potable supply for communities around the world.[27] Thus, growing concern regarding the migration of PFAS from ground to drinking water sources is becoming a pressing issue for public health and environmental safety. This aspect is further reinforced by recent data demonstrating that even low concentrations of PFAS can exert detrimental effects on human health, including immune system dysfunction and increased cancer risk.[28,29]

To address the toxicity of PFAS, we recently proposed the medicinal leech *Hirudo verbana* (*H. verbana*) as a model organism to investigate its impact on innate immunity and angiogenesis. Unlike traditional invertebrate models such as *Drosophila melanogaster* or *Caenorhabditis elegans*, *H. verbana* possesses a closed circulatory system, circulating immune cells, and vascular-like structures resembling those of vertebrates,[30,31] enabling biologically relevant studies on inflammation, oxidative stress, and vascular remodeling. Its immune system includes conserved components analogous to vertebrate responses, as confirmed by transcriptomic analyses showing high similarity between leech innate-immune genes and mammalian counterparts.[32] Prior studies have shown that *H. verbana* responds to environmental contaminants with upregulation of proinflammatory markers (e.g., *Hv*RNASET2, *Hm*AIF-1, and IL-18),[33,34] increased oxidative stress (*SOD* and *GST*),[35] ROS production,[36] and activation of phagocytosis and angiogenesis,[37,38] supporting its use as a sentinel species. Moreover, vertebrate antibodies such as CD11b, CD45, CD68, CD31, and VEGF receptors (Flt-1/VEGFR-1 and Flk-1/VEGFR-2) cross-react with leech tissues, indicating conserved epitopes involved in immune and vascular processes[31,33,39−41] and enabling immunohistochemical investigation using vertebrate tools. These features highlight *H. verbana* as an ecologically relevant and experimentally versatile invertebrate model for assessing pollutant-induced alterations to the immune homeostasis and vascular integrity.

In previous work, we showed that a 24 h exposure to PFOA and C4−C6 short-chain perfluoro ether carboxylic acids at different concentrations (0.6 and 299 μmol L^{-1}) triggered acute inflammation in *H. verbana*. Notably, next-generation PFAS congeners like HFPO-DA, PFMOPrA, and PFMoBa elicited toxicological profiles comparable to PFOA.[35]

Here, we test whether structurally distinct PFAS, PFOA, straight-chain perfluoro carboxylic acids (PFCAs) versus the ether compounds (HFPO-DA, PFMOPrA, and PFMoBa) differing in perfluoroalkyl length (C4−C8) and ether position (α vs β/γ) sustain innate-immune and angiogenic alterations and influence regeneration, under chronic, environmentally realistic exposure, aligning our design with the EU Drinking Water Directive parameters used by Member States for compliance (PFAS total = 0.50 μg L^{-1}). Compared to PFOA, HFPO-DA is a short-chain ether replacement produced during fluoropolymer manufacture and widely reported in impacted waters in North America, Europe, and China. The closest low-carbon analogues of HFPO-DA are PMPA (perfluoro-2-methoxypropanoic acid) and PEPA (perfluoro-2-ethoxypropanoic acid), which share its α-alkoxy (branched) topology; however, commercially available standards for PMPA/PEPA were not commercially available at study design. We therefore employed the isomeric methoxy-PFECAs PFMOPrA (C4, $-OCF_3$) and PFMoBa (C5, $-OCF_3$), both reported alongside HFPO-DA in the Cape Fear River (NC, USA) watershed, including finished drinking water, consistent with coproduced impurities/byproducts in fluoropolymer production streams.[42,43] Notably, monitoring reports sometimes group methoxy-PFECAs and do not always resolve positional/branched isomers.[44] In China, PFECAs are increasingly reported in surface waters and drinking water systems near fluorochemical hubs (e.g., Poyang Lake; lower Yangtze), with HFPO-DA and methoxy-PFECAs prominent, and PFECA bioaccumulation documented in estuarine food webs, supporting exposure plausibility for this structural class.[45−47] By pairing PFMOPrA (C4) and PFMoBa (C5), we introduce a one-CF_2 increment at a conserved ether headgroup, while HFPO-DA provides a larger heptafluoropropoxy ether; together with PFOA, this panel allows us to probe how the perfluoroalkyl length and ether size/position govern chronic innate-immune and angiogenic outcomes. To this end, we exposed leeches to 1 nmol L^{-1} of each compound for two months (acid-equivalent ≈ 0.23−0.41 μg L^{-1} across analytes, see Section 2.1). This anchors our comparisons to concentrations that are policy-salient and within the upper end of PFAS levels intermittently observed in European freshwaters and groundwater near emission sources.

2. MATERIALS AND METHODS

2.1. Animals and Treatments

Medicinal leeches (*H. verbana*, Annelida, and Hirudinea), derived from the ILFARM breeding (Italian Leech Farm, Italy), were maintained in aerated tanks in 200 mL of slightly salted water (1.5 g L^{-1} NaCl) at 20 °C. For the treatments, adult animals (10 cm in length) were randomly separated into distinct experimental groups and exposed to diverse treatments. For each condition, defined by the specific PFAS used, a total of five animals were used, and all of the experiments were performed in triplicate. After 2 months from PFAS water administration, leeches were anesthetized in a 10% ethanol solution until they appeared completely asleep and then sacrificed.

Group 1: Leeches were exposed to isopropyl alcohol [$(CH_3)_2CHOH$] (0.005%) and used as a control. The same isopropanol concentration was also used to dilute the PFAS tested. Control experiments were necessary to dismiss any possible side effects induced by this chemical.

https://doi.org/10.1021/envhealth.5c00268
Environ. Health XXXX, XXX, XXX−XXX

Groups 2: Leeches were treated for 2 months with ammonium perfluoro(2-methyl-3-oxahexanoate) (HFPO-DA).

Groups 3: Leeches were treated for 2 months with perfluoro-4-methoxybutanoicacid (PFMoBa).

Groups 4: Leeches were treated for 2 months with perfluorooctanoic acid (PFOA).

Groups 5: Leeches were treated for 2 months with perfluoro-3-methoxypropanoic acid (PFMOPrA).

The animals' water was changed weekly in order to maintain a consistent concentration of PFAS. Moreover, the precise concentrations of PFAS were selected to evaluate the long-term effects, within the framework of an EU project on PFAS (https://scenarios-project.eu). To this aim, we selected 1 nmol L^{-1} to reflect the upper end of policy-relevant drinking water levels in the EU. At this molarity, mass concentrations span ≈0.33−0.414 μg L^{-1} across the PFAS tested (PFMOPrA ≈ 0.230 μg L^{-1}; PFMoBa ≈ 0.280 μg L^{-1}; HFPO-DA ≈ 0.330 μg L^{-1}; PFOA = 0.414 μg L^{-1}), placing our exposure near the 0.50 μg L^{-1} "PFAS total" parameter and above the 0.10 μg L^{-1} "sum of PFAS" threshold used by UE Member States. Furthermore, reported European surface and groundwaters are typically in the ng L^{-1} range, with local hotspots occasionally reaching 10^2−10^3 ng L^{-1},[25,26] supporting the realism of our chronic test level for organisms inhabiting impacted waters.

In vivo studies were conducted using medicinal leeches of the species *H. verbana*, which are not protected under Directive 2010/63/EU governing the use of animals in scientific research, nor are they listed in Legislative Decree no. 26, of 4 March 2014, "Implementing Directive 2010/63/EU on the protection of animals used for scientific purposes", published in the Italian Official Journal on 14 March 2014. However, their use has been authorized by the Animal Welfare Body (OPBA) at the University of Insubria.

2.2. Tissue Sampling

Small fragments were collected from the animals to perform the different analyses. Leeches exhibited a consistent body structure along their entire length with similar anatomical features observable across sections, except for the more apical cephalic and posterior regions. This uniformity allowed multiple samples to be obtained from the same animal, providing adequate biological material for all of the planned experiments.

2.3. Optical Microscopy Analyses

Leech samples used for morphological analysis, including quantitative assessment of vessel and granulocyte numbers, were collected and fixed in 4% glutaraldehyde (diluted in 0.1 mol L^{-1} cacodylate buffer, pH 7.4) at room temperature for 2 h. After three washings in the same buffer, samples were postfixed for 1 h in the dark using 2% osmium tetroxide (OsO_4). Subsequently, tissues were washed again in cacodylate buffer and then dehydrated with an increasing ethanol concentration (30, 50, 70, 90, 96, and 100%). Samples were transferred into a solution of propylene oxide and resin (1:1 ratio) for 1 h and last embedded in an Epon-Araldite 812 mixture epoxy resin (Sigma-Aldrich, Italy). Semithin sections for light microscopy (750 nm) were obtained with an RMC PowerTome XL (Boeckeler Instruments, USA), collected on a slide, and stained with crystal violet (1 g in 100 mL of distilled water) and basic fuchsin (0.13 g in 100 mL of distilled water). Samples were finally observed under a light microscope (Eclipse Nikon, Japan), and data were recorded with a DS-5M-L1 digital camera system (Nikon, Japan).

2.4. Immunofluorescence Assay on Cryosections

All samples were rapidly included into an OCT (optimal cutting temperature compound) (Polyfreeze TebuBio, France), frozen in liquid nitrogen, and stored at −80 °C. Cryosections (7 μm) were obtained with a cryostat (Leica CM1850), collected on gelatinated slides (coated with bovine serum albumin, BSA), and held at −20 °C. Sections were then rehydrated for 10 min in PBS (138 mmol L^{-1} NaCl, 2.7 mmol L^{-1} KCl, and 4.3 mmol L^{-1} Na_2HPO_4, pH 7.4) and incubated in the BSA blocking solution (2% BSA, 0.1% Tween diluted in PBS) for 30 min and then for 1 h at room temperature with the primary antibodies (Table 1) (BSA was used to dilute both primary and secondary antibodies). These specific primary antibodies were already used in leeches to specifically detect endothelial cells,[35,41,48] or granulocytes[49] or hematopoietic precursors cells and their derived monocyte-macrophage-like cell populations.,[40,50] After several washes in PBS buffer, slides were incubated with suitable secondary antibodies conjugated with fluorescein isothiocyanate (FITC, Thermo Fisher Scientific, dilution 1:250) for 45 min. Nuclei were then counterstained with 4,6-diamidino-2-phenylindole (DAPI) 0.1 mg mL^{-1} diluted in PBS for 5 min, and slides were mounted with PBS/Glycerol Cityfluor (Cityfluor, UK). Negative control experiments were performed by omitting primary antibodies. All samples were examined with a fluorescence microscope (Nikon Digital Sight DS-SM, Japan), and staining was visualized using excitation/emission filters of 490/525 nm for FITC and 340/488 nm for DAPI. The obtained images were then combined using Adobe Photoshop (Adobe System, Inc.).

Table 1. List of the Primary Antibodies

antibodies	description	company	application	dilution
CD31	rabbit polyclonal	Abcam	IF	1:100
CD11b	rabbit polyclonal	Santa Cruz Biotechnology, Inc.	IF	1:100
CD45	rabbit polyclonal	GenScript	IF	1:200
VEGF-R2	mouse monoclonal	Sigma-Aldrich	IF	1:50

2.5. Acid Phosphatase (ACP) Assay

Cryosections were rehydrated in PBS physiological solution for 10 min and incubated for 5 min in 0.1 mol L^{-1} acetic acid-sodium acetate buffer and then at 37 °C with the reaction mixture (sodium acetate-acetic acid buffer (0.1 mol L^{-1}), 0.01% naphthol phosphate, 2% N,N-dimethylformamide, 0.06% Fast Red, and $MnCl_2$ (0.5 nmol L^{-1})) for 90 min. After five washings in the same physiological buffer, samples were mounted with Cityfluor (Cityfluor, UK) hydrophobic mounting and observed under a light microscope, and data were recorded as described above.

2.6. Paraffin Inclusion and Mucus Cell Analysis by Histochemical Staining PAS (Periodic Acid−Schiff)

For paraffin inclusion, samples were fixed with 4% paraformaldehyde. Following 5 washes in PBS, tissues were dehydrated using an increasing concentration of ethanol (30, 50, 70, 90, 96, and 100%), transferred to a paraffin and xylol solution (1:1 ratio) overnight, and finally included in paraffin. Then, samples were cut with a microtome (Jung 2045, Leica), and collected sections (0.7 μm in thickness) were processed for the PAS histochemistry reaction, as recommended by the seller's instructions (PAS kit, Bio Optica, Italy). This staining allows to observe and characterize the mucus cells present in the leech tissue, as already described.[34] Samples were then observed under the light microscope, and the images were acquired as described above.

2.7. RNA Extraction and Quantitative Polymerase Chain Reaction (qPCR)

For the RNA extraction and qPCR analyses, all of the animals involved in the study were processed. Entire leech body wall sections (30 mg, wet weight) were instantly frozen in liquid nitrogen and homogenized with a pestle and mortar, further resuspended and lysed in 1 mL of a Trizol reagent (Thermo Fisher Scientific, USA) by multiple pipetting, with total RNA extracted according to the manufacturer's instructions, and finally resuspended in 30 μL of RNase-free water. Samples were then quantified using a NanoDrop spectrophotometer (Thermo Fisher Scientific, USA), and the RNA purity was evaluated by means of high-resolution 1.5% agarose gel electrophoresis under denaturing conditions. 2 μg of RNA was retrotranscribed into cDNA using M-MLV reverse transcriptase (Thermo Fisher Scientific, USA) in the presence of oligodT (Invitrogen, Thermo Fisher Scientific, USA; length: 16 bp) in a final volume of 20 μL. Quantitative real-time PCR (qPCR) was carried out in triplicate in a CFX Connect Real-Time PCR detection system (Bio-Rad, USA) using an iTaq Universal SYBR master mix (Bio-Rad, USA) and 0.2 μmol L^{-1} each of forward and reverse

https://doi.org/10.1021/envhealth.5c00268
Environ. Health XXXX, XXX, XXX−XXX

Table 2. List of Primers Used for qPCR Analyses

target genes	product size (bp)	primers	*T* melting (°C)
*Hv*RNASET2	136	fw: 5′-GGTCCCAACTTCTGCACAAAGGAT-3′	58.3
		rev: 5′-GTTTGTCCCATTCATGCTTCCAGAA-3′	58.5
*Hm*AIF-1	229	fw: 5′-GACCTCAAAGACAAGCAGGG-3′	57.7
		rev: 5′-GGCCAATCTTCTCCAGCATC-3′	58.5
GST	127	fw: 5′-AGACACATCGCCAGGACTAA-3′	58.4
		rev: 5′-ACGGATACACGACTCCAACT-3′	58.5
SOD	95	fw: 5′-ATCCTCTTGAACCCACCACA-3′	58.6
		rev: 5′-ATCTGGACGCACATTCTTGT-3′	58.7
GAPDH	121	fw: 5′-GAAGACTGTGGATGGACCCT-3′	58.7
		rev: 5′-GTTGAGGACTGGGATGACCT-3′	58.7

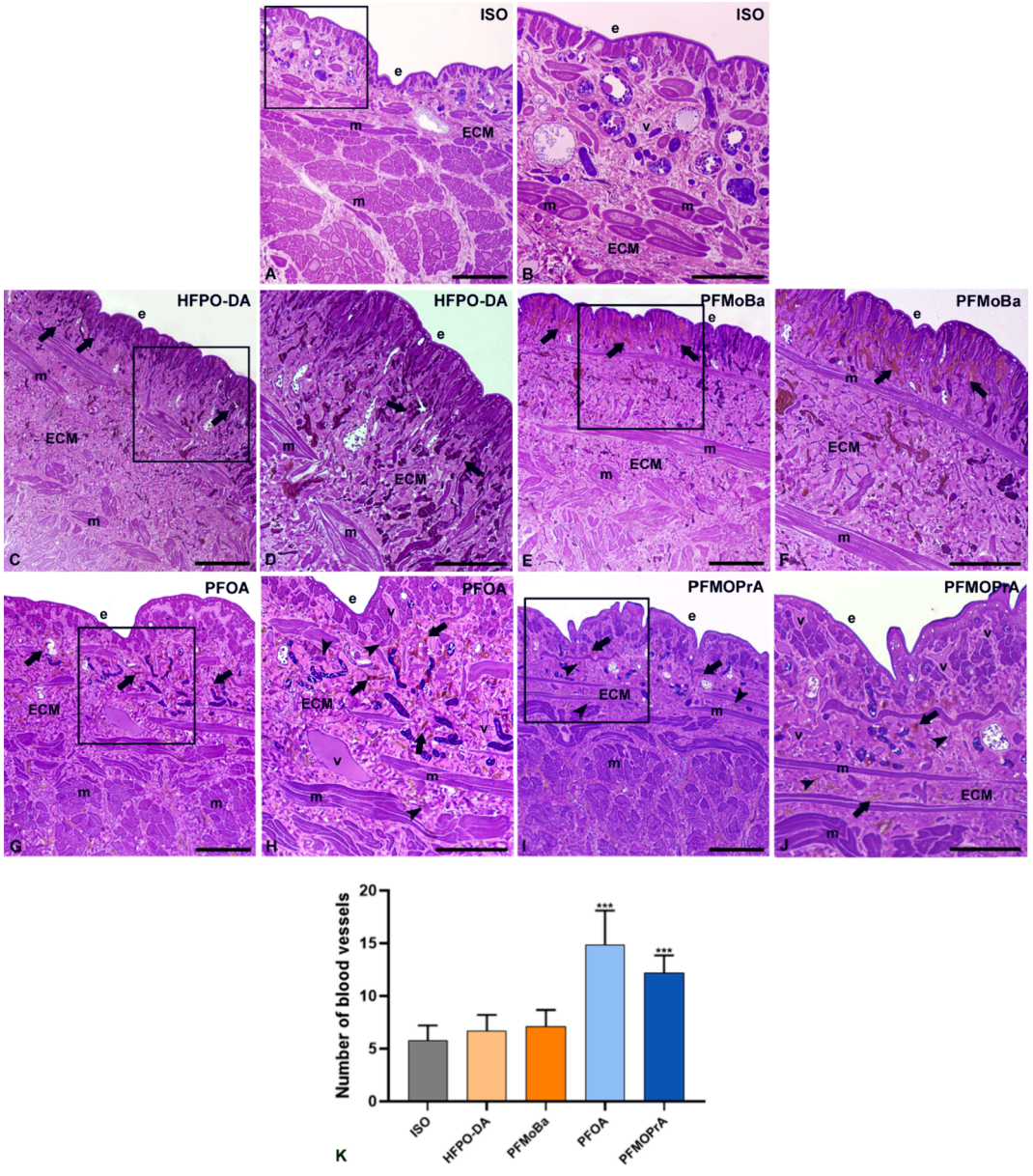

Figure 1. Morphological analyses of leeches exposed to isopropanol, used as control (A, B), and to the different PFAS compounds (C–J). Details at higher magnification of isopropanol-treated (B) and PFAS-treated (D–J) samples are referred to black squares. The graph indicates the number of blood vessels observed by means of morphological analyses in different treated samples (K). Bars in A, C, E, G, and I: 100 μm; bars in B, D, F, H, and J: 50 μm. ECM: extracellular matrix; e: epithelium; m: muscles; v: blood vessels; arrowheads: macrophages; arrows: granulocytes.

primers, in final a volume of 15 μL. After initial denaturation, the PCR reaction was performed at 95 °C (10 s), 60 °C (5 s), and 72 °C (10 s) for 39 cycles. Relative gene expressions were calculated using the ΔΔCt method, and *GAPDH* (D-glyceraldehyde-3-phosphate dehydrogenase)

https://doi.org/10.1021/envhealth.5c00268
Environ. Health XXXX, XXX, XXX−XXX

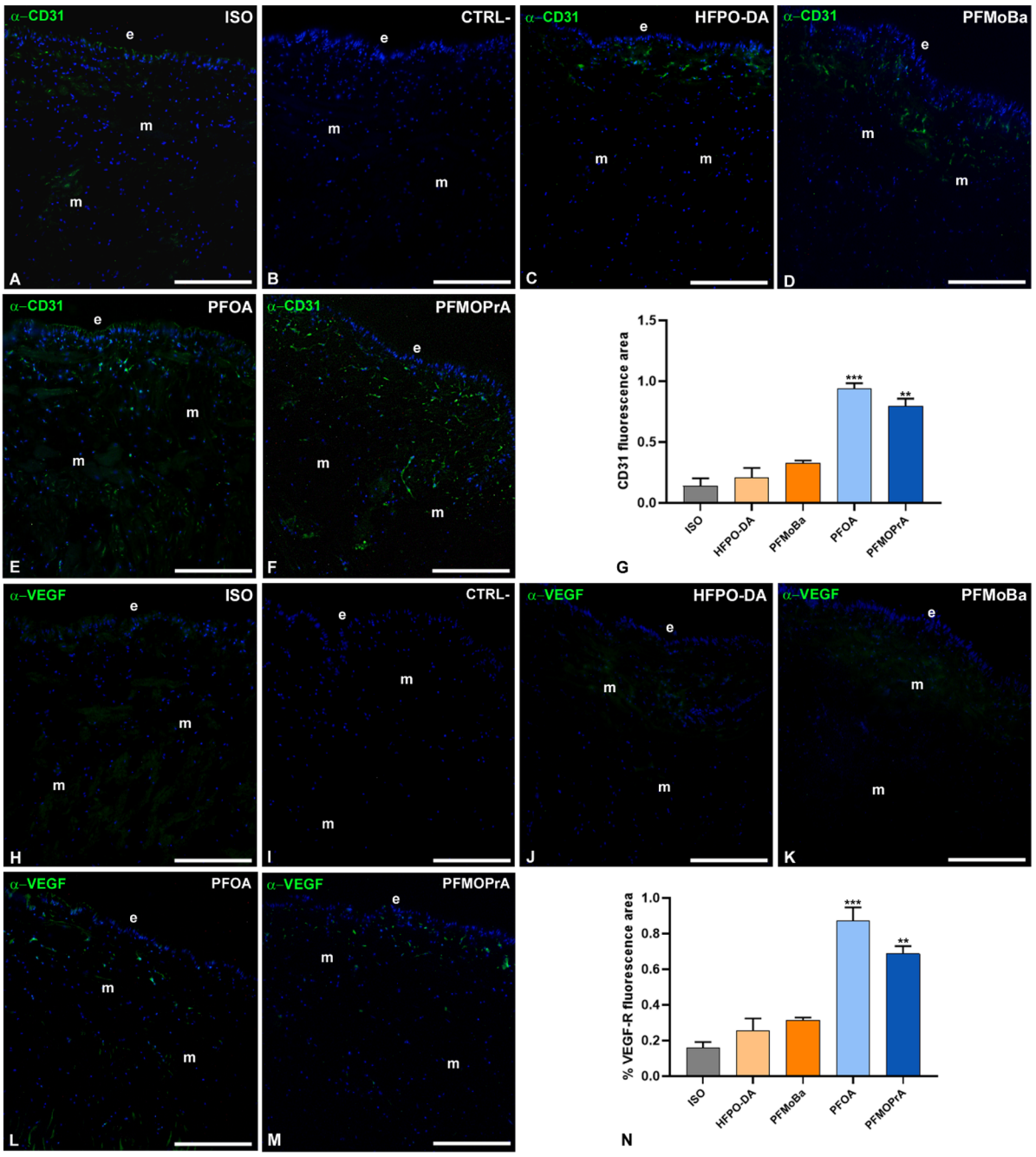

Figure 2. Evaluation of angiogenic process induction after PFAS chronic exposure (A–G). Immunofluorescence analyses using specific anti-CD31 and VEGF-R2 antibodies (B–E). As expected, an increase in both fluorescent signals is mainly visible only after PFOA (F, L) and PFMOPrA (G, M) treatments compared to the control (A, H) and HFPO-DA (D, J) or PFMoBa (E, K) exposure. Cell nuclei are stained with DAPI, and no signals are visible in negative control experiments, in which the primary antibody is omitted (C, I). The graphs indicate the CD31 and VEGF-R2 total fluorescent areas in different treated samples (G, N). Bars in B–G: 100 μm. e: epithelium; m: muscle fibers.

was used as a reference gene. The primers used for qPCR amplifications are reported in Table 2. All of the primer sequences possessed an amplification efficiency of 99%, and the melt curve was assessed.

2.8. Statistical Analyses

The statistical analyses were conducted using Prism GraphPad 8 software (GraphPad Software, USA), and significant differences were calculated by means of one-way ANOVA after verification of normality and homoscedasticity by means of Shapiro–Wilk and Levene tests, respectively. Significant differences were calculated followed by Dunnett's *post hoc* test, and values of $p < 0.05$ were considered statistically significant. In the graphs, averages ± standard deviation (SD) with asterisks represented the significant differences between vehicle control animals and PFAS-treated leeches. For blood vessels, granulocytes, APC$^+$ macrophages, both type 1 and type 2 mucus cell total count, and CD45 fluorescent signal intensity evaluation, 10 different slides (random fields of 45.000 μm^2 for each) were analyzed using the ImageJ software package (Bethesda, USA). All image acquisitions and quantifications were performed blindly to minimize observer bias.

https://doi.org/10.1021/envhealth.5c00268
Environ. Health XXXX, XXX, XXX–XXX

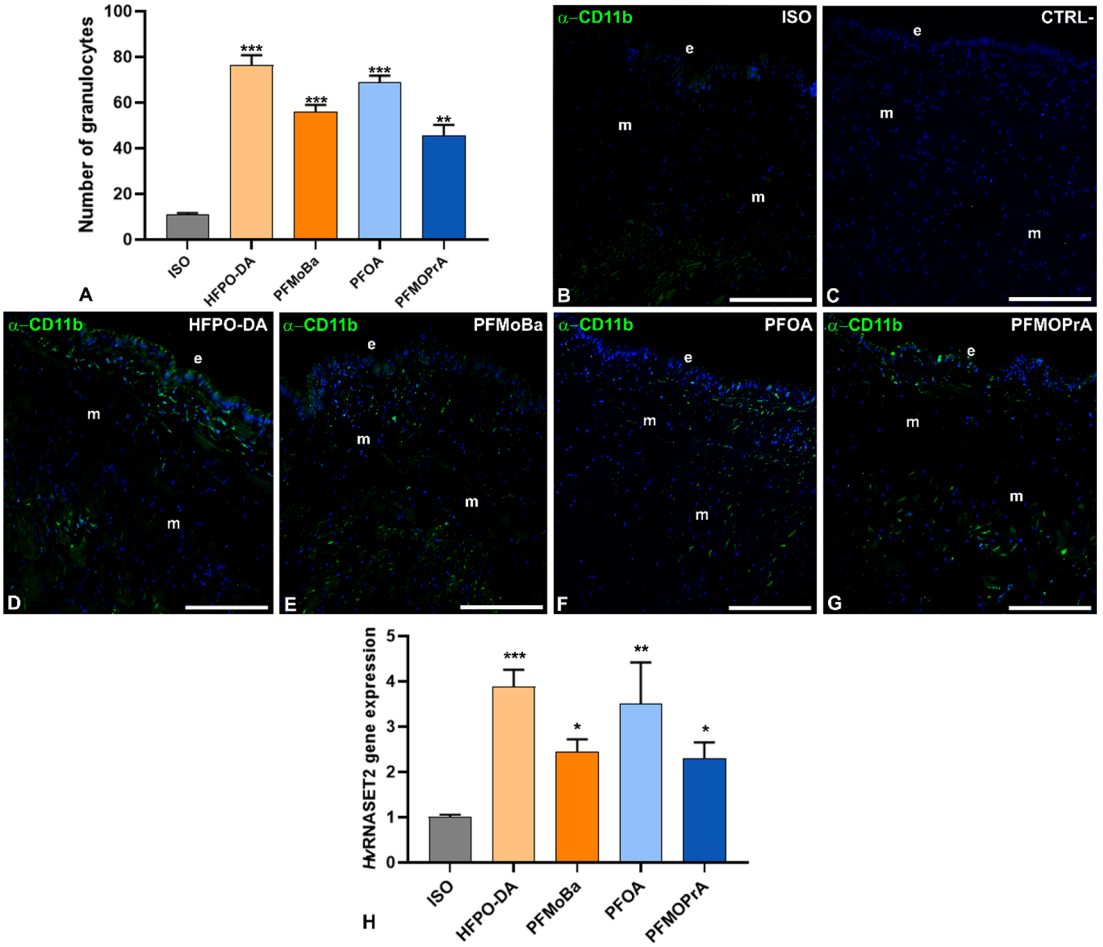

Figure 3. Quantification and characterization of granulocytes recruited after PFAS chronic exposure (A–E). The graph indicates the number of granulocytes observed in morphological analyses in different treated samples (A). Immunofluorescence analyses used the anti-CD11b antibody (B–E). As expected, an increase in the number of granulocytes is visible in all samples, with more significant results in HFPO-DA (D), PFOA (F) and PFMoBa (E) samples, compared to the control. Cell nuclei are stained with DAPI, and no signals are visible in negative control experiments, in which the primary antibody is omitted (C). *Hv*RNASET2 qPCR analyses (H). Bars in B–G: 100 μm. e: epithelium; m: muscle fibers.

3. RESULTS

3.1. Morphological Evaluation of Leech Tissues Exposed to PFAS

The effects induced by chronic PFAS exposure were primarily evaluated through morphological analyses (Figure 1). Optical microscopy images showed that the body wall of isopropanol-treated leeches, used as controls, displayed a typical condition similar to that of untreated animals. The tissues appeared largely avascular, with only a few immune cells present, located either underneath the epithelium or within the inner muscle layer (Figure 1A,B). In contrast, several remarkable differences were detected following PFAS treatment (Figure 1C–H), with significant variations based on the fluorinated compounds tested. Compared to control samples (Figure 1A,B), numerous newly formed blood vessels were observable in leeches treated with PFOA and PFMOPrA (Figure 1G–J), whereas no such evidence was found in those exposed to HFPO-DA and PFMoBa (Figure 1C–F). Interestingly, different outcomes were also observed in the modulation of the innate-immune system responses. Indeed, although a significant recruitment of leech granulocytes occurred in all examined samples, with a higher concentration in those treated with HFPO-DA and PFOA (Figure 1C,H), the activation of macrophage-like cells, localized underneath the epithelium and in the muscular body, was evident only after PFOA and PFMOPrA exposure (Figure 1H,J), suggesting differential activation of leech immune cell populations according to the specific fluorinated molecule tested. In addition, morphometric analysis of vessel density showed that vessel density remained unchanged in leeches exposed to the vehicle (isopropyl alcohol), HFPO-DA, or PFMoBa. In contrast, a significant increase was observed following exposure to PFOA and PFMOPrA (Figure 1K).

3.2. Characterization of Angiogenic Events

Immunofluorescence assays targeting anti-CD31 and anti-VEGF-R2, specific endothelial markers in *H. verbana* (Figure 2), were performed to analyze PFAS-induced angiogenic activation. Both CD31 and VEGF-R2 immunofluorescence displayed consistent patterns: the signal was negligible in sections from leeches treated with vehicle, HFPO-DA, and PFMoBa (Figure 2A,C,D,H,J,K), whereas a 3- to 4-fold intensification was detected in PFOA- and PFMOPrA-exposed animals, particularly beneath the epithelium and between muscle fibers (Figure 2E,F,L,M). No signals were detected in control sections incubated without the primary antibody, confirming the specificity of the staining (Figure 2B,I). These findings indicate that only PFOA and PFMOPrA among the tested PFAS elicit a robust angiogenic response in *H. verbana*, as

https://doi.org/10.1021/envhealth.5c00268
Environ. Health XXXX, XXX, XXX–XXX

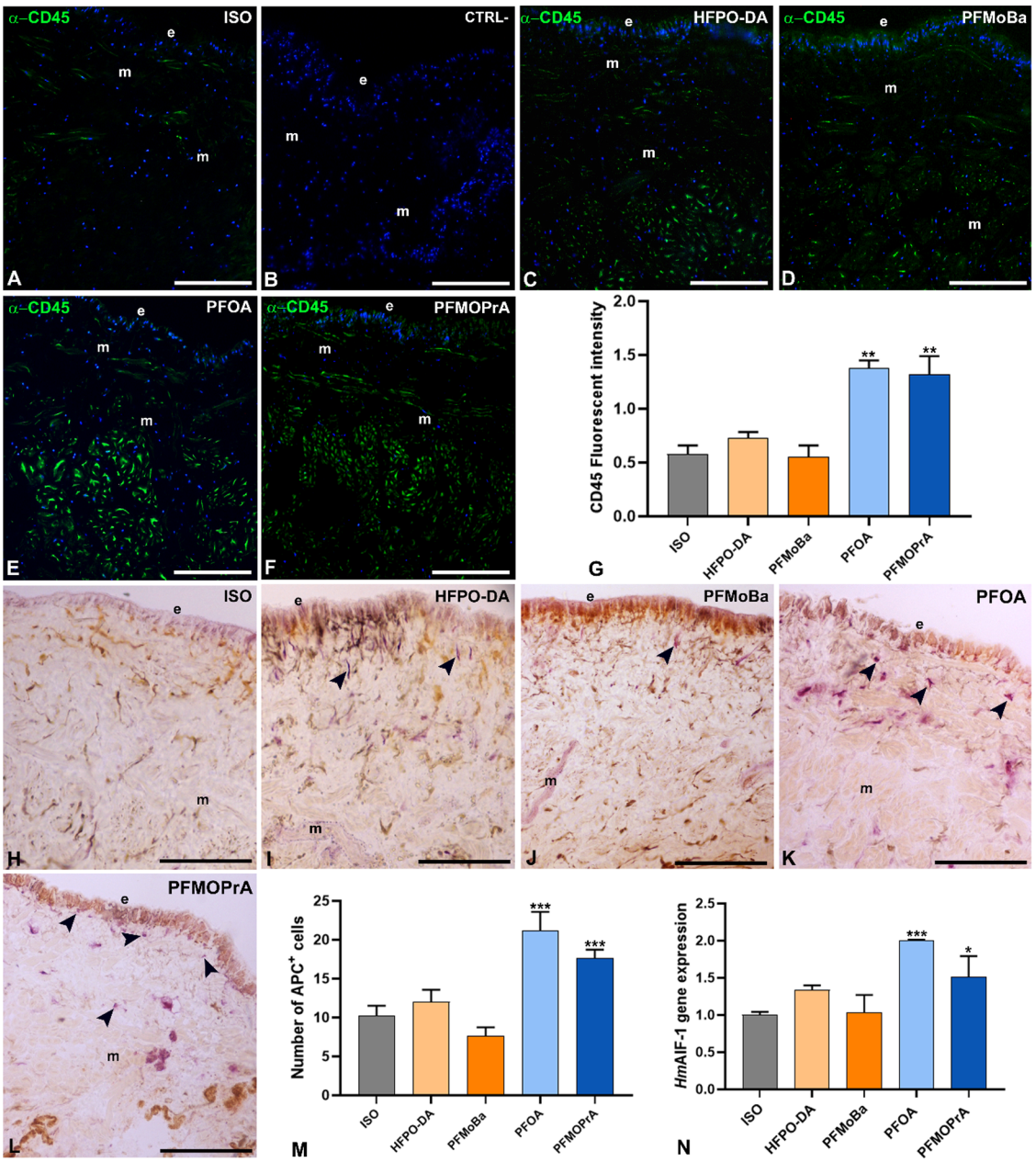

Figure 4. Immunofluorescence analyses of isopropanol control and PFAS-treated leeches using an anti-CD45 antibody (A−H), specific for the leech monocyte-macrophage-like cell lineage. In untreated (A), HFPO-DA- (C), and PFMoBa-treated (D) leech tissues, only a few CD45$^+$ cells are decorated, while an increase in the signal becomes clearly detectable only after PFOA (E) and PFMOPrA (F) chronic treatments, as reported in the graph related to the total fluorescent signal calculated (G). Cell nuclei are stained with DAPI, and no signals are visible in negative control experiments, in which the primary antibody is omitted (B). Acid phosphatase assay (ACP) to evaluate recruited active macrophages during chronic PFAS response (H−M). The data reveal that, compared to the control (H), HPFO-DA (I), and PFMoBa (J) in which no significant differences are visible, an increase in ACP$^+$ cells (thin arrows) is visible after PFOA (K) and PFMOPrA (L) exposure. The count of ACP-positive cells is reported in a graph (M). The graph (N) shows the *Hm*AIF-1 expression profile in isopropanol control tissues of leeches or in animals treated with PFAS. Bars in A−F and H−L: 100 μm. e: epithelium; m: muscle fibers.

demonstrated by the increased levels of CD31 and VEGF-R2 expression, as observed in the graph (Figure 2G,N).

3.3. Quantification and Characterization of Immunocytes Involved in the Innate-Immune Response Triggered by PFAS Exposure

3.3.1. Leech Granulocyte Quantification and Characterization. As shown in Figure 3A, the chronic PFAS chronic exposure led to a significant increase in granulocyte numbers across all exposed samples, compared to the isopropanol-treated animals. This result was further validated by immunofluorescence (Figure 3B−G) using the leech granulocyte-specific marker CD11b.[34] Fluorescent images demonstrated a clear increase in CD11b$^+$ cells in all PFAS-exposed samples compared to the controls (Figure 3D−G). No fluorescent signal was detected in the negative control experiments, where the primary antibody was omitted (Figure 3B), confirming the staining specificity. To further investigate the PFAS ability in activating leech granulocytes, also the expression of the *Hv*RNASET2 proinflammatory marker was evaluated by means of qPCR (Figure 3H). The data revealed that the *Hv*RNASET2

https://doi.org/10.1021/envhealth.5c00268
Environ. Health XXXX, XXX, XXX−XXX

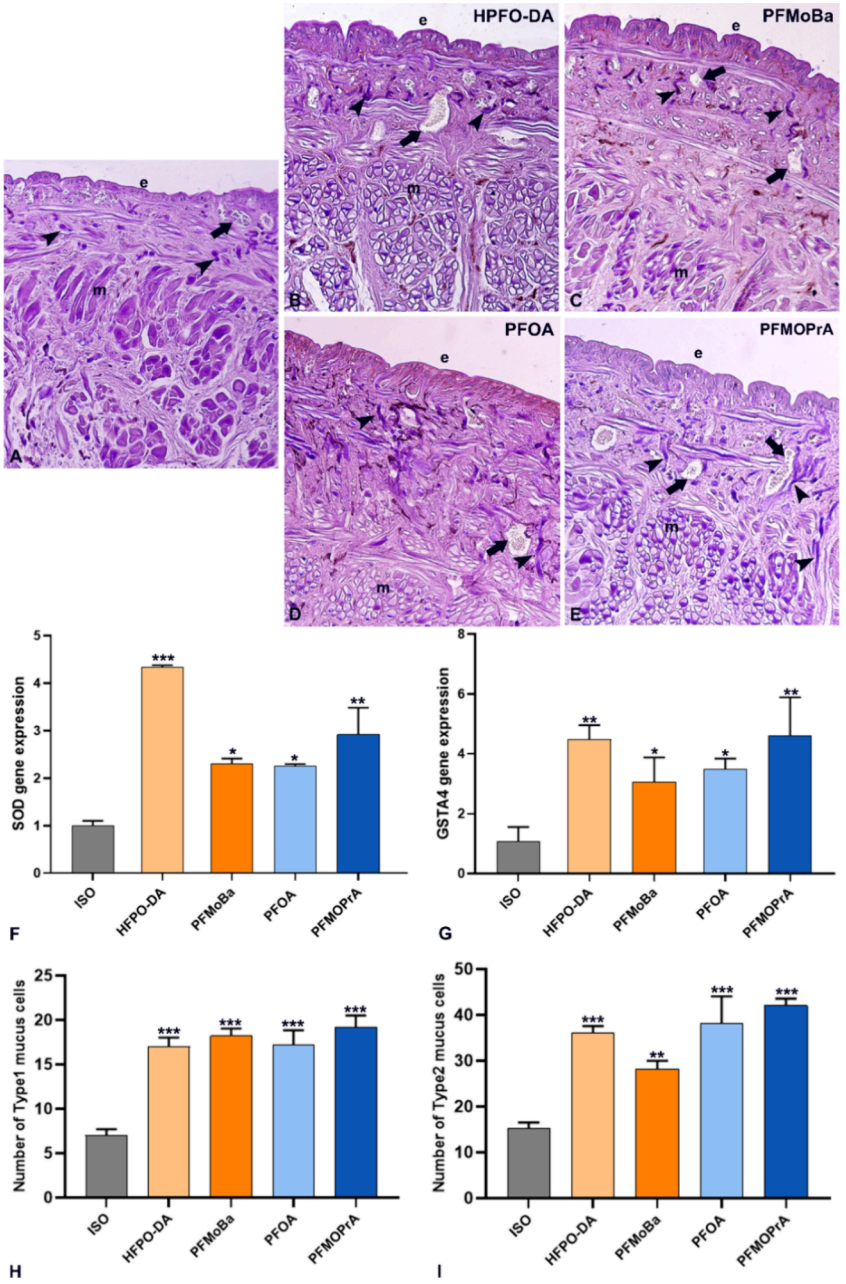

Figure 5. Evaluation of the oxidative stress response. In control samples (A), type 1 (arrows) and type 2 (arrowheads) mucus cells are characterized by a rounded shape inactive form and are located under the epithelium (e) and between the muscle fibers (m). After PFAS administration (B–E), especially type 2 cells appear more elongated, suggesting a continued stimulation. Expression of *SOD* and *GST* was examined by qPCR analyses (F, G). The graphs show the expression levels of both oxidative enzymes in isopropanol control leeches or in leeches treated with PFAS. The total number of both type 1 and type 2 mucus cells was quantified, and the differences between treatments are illustrated in the corresponding graphs (H, I). Bars in A–F: 100 μm.

expression levels were higher in all treated samples compared to controls. Of note, the expression trend of *Hv*RNASET2 mirrored the number of leech granulocytes recruited to the area exposed to PFAS, thus confirming previous findings.[49]

3.3.2. Monocyte-Macrophage-like Cell Characterization and Quantification. The recruitment of both leech circulating hematopoietic precursor cells and their derived monocyte-macrophage-like cell populations was primarily assessed through immunofluorescence analyses (Figure 4). In particular, a reduced CD45^{+} cell number was observed in control animals (Figure 4A), as well as in leeches treated with HFPO-DA (Figure 4C) and PFMoBa (Figure 4D). In contrast, a significant increase in the CD45 fluorescent intensity was detected after PFOA and PFMOPrA exposure (Figure 4E,F). No signals were observed in the negative control experiments in which the primary antibody was omitted (Figure 4B). These findings, corroborated by the quantitative analysis of total CD45 fluorescence (Figure 4G), indicated a different potency of PFAS in modulating monocyte-macrophage inflammatory pathways. Notably, this finding was in line with the reduced level of neovascularization previously observed in HFPO-DA- and PFMoBa-treated samples (Figure 1C–F).

Macrophage-like cell activation by PFOA and PFMOPrA was confirmed via the acid phosphatase (ACP) enzymatic assay

https://doi.org/10.1021/envhealth.5c00268
Environ. Health XXXX, XXX, XXX–XXX

(Figure 4H−M) and qPCR analyses (Figure 4N). As expected, few ACP$^+$ cells were detectable after isopropanol (Figure 4H), HFPO-DA (Figure 4I), and PFMoBa (Figure 4C) exposure. Meanwhile, after the treatment with PFOA (Figure 4K) and PFMOPrA (Figure 4L), their number significantly increased, both underneath the epithelium and in the inner muscle layers, as also reported in the graph related to the total ACP-positive cell count (Figure 4M). In parallel, the expression level of the *Hm*AIF-1 cytokine, specifically involved in macrophage-like cell recruitment, was analyzed (Figure 4N). The qPCR data revealed that *Hm*AIF-1 was significantly expressed only in samples exposed to PFOA and PFMOPrA, confirming the strong activation of ACP$^+$ macrophage-like cells in these samples.

3.4. Evaluation of the Oxidative Stress Response

The ability of PFAS to induce oxidative stress was evaluated by examining both the activation of leech type 1 and type 2 mucus cells and the expression levels of two fundamental antioxidant enzymes: the superoxide dismutase (*SOD*) and the glutathione-*S*-transferase (*GST*) (Figure 5).

In detail, histochemical analyses revealed that in control samples, few type 1 and type 2 mucus cells presenting the distinctive round shape of nonactivated secretory cells were present close to the epithelium (Figure 5A). Instead, following PFAS exposure (Figure 5B−E), both their morphology and number increased considerably (Figure 5H,I). Indeed, numerous elongated mucus cells, stretching toward the inner muscle and the epithelial layer, were clearly visible. In parallel, qPCR assays revealed that the expression of *SOD* and *GST* was significantly higher in all PFAS-treated samples compared to the controls (Figure 5F,G).

4. DISCUSSION

In the current study, we chose four PFAS compounds that include both older and newer chemistries, thus comparing their structure−activity relationships at the same policy-relevant dose. Although acute exposure studies are essential to identifying the immediate effects of pollutants, they are often insufficient to capture delayed or cumulative outcomes. Many contaminants persist in the environment, bioaccumulate in organisms, and may induce harmful effects only after prolonged exposure. Moreover, physiological and morphological alterations often develop gradually as organisms initially compensate for stress. For this reason, assessing long-term impacts is crucial to fully understand the toxicological profile of a compound.[51,52]

Consistent with this, the data collected in this work demonstrate that fluorinated compounds elicit chronic responses distinct from those observed after acute exposure, underscoring the need for a broader long-term perspective on their toxic potential. Specifically, our earlier investigation showed that, regardless of the dose chain length or functional group, all PFAS tested triggered an inflammatory sequence in *H. verbana* comprising an initial influx of CD11b$^+$ granulocytes, recruitment of CD45$^+$ macrophage-like cells, and CD31$^+$ and VEGF-R2$^+$ angiogenesis.[35] However, this cascade remains intact for PFOA and PFMOPrA throughout two months of exposure at 1 nmol L^{-1}, whereas for HFPO-DA and PFMoBa, it stalls at the granulocyte phase, with no subsequent macrophage recruitment or vascular remodeling. These contrasting outcomes confirm that prolonged interactions at environmentally relevant concentrations can either consolidate or blunt the toxicological profiles of individual PFAS.

From a risk perspective, the finding that 1 nmol L^{-1} (acid-equivalent ≈ 0.23−0.41 μg L^{-1} across analytes; e.g., PFOA at 0.414 μg L^{-1}) can sustain innate-immune activation over two months is noteworthy in light of the current European policy. The EU Drinking Water Directive [Directive (EU) 2020/2184] requires Member States to ensure compliance by January 12, 2026 with parametric values of 0.10 μg L^{-1} for the sum of PFAS or 0.50 μg L^{-1} for the PFAS total. Our test level lies near the latter threshold for several PFAS and overlaps the upper range of concentrations sometimes detected in European surface and groundwaters near contamination sites.[24−26] Thus, the tissue-level alterations that we document are plausibly encountered by organisms inhabiting contaminated waters and remain mechanistically relevant to human water-quality management.

Although PFMOPrA and PFMoBa differ minimally in chemical structure, our findings clearly show that even subtle variations in the molecular architecture can result in distinct biological outcomes. PFMOPrA behaves similarly to PFOA, sustaining the full CD11b/CD45/CD31/VEGF-R2 inflammatory cascade, while PFMoBa blocks the process after the granulocyte stage. Such divergence likely stems from structural differences that influence physicochemical behavior, cellular uptake, bioaccumulation, or interference with immune-related signaling pathways.

As for PFOA, no specific differences are visible when comparing previous short timings and the current results. Its prominent role in driving immune-related alterations is confirmed also over longer exposure in treated leeches, demonstrating that this legacy PFAS is certainly one of the most unsafe molecules, able to trigger considerable harmful effects in various organisms.[53,54] For this reason, its production has been banned or extremely globally restricted, especially for its proven carcinogenic potential.[52] Similar to the evidence recorded during the acute response, PFOA causes a severe inflammation in aquatic invertebrates also after a prolonged contact. Consistent with the canonical cascade, granulocytes labeled by CD11b accumulate first, followed by a robust influx of CD45$^+$ macrophage-like cells and, finally, a CD31- and VEGF-R2-positive neovascularization beneath the epithelium and within the inner muscle layer. Indeed, light microscopy images show a high activation of these cells, which migrate toward the external layers following recruitment by the entry of this fluorinated compound, increasing in number, as also confirmed by immunofluorescent, histochemical enzymatic, and molecular assays. In this context, the vascular formation is critical to facilitate the continuous recruitment of hematopoietic precursor cells that migrate through the circulatory system into the target area and differentiate into mature effector immune cells.[55,56]

High CD11b fluorescence identifies the granulocyte wave, strong CD45 staining and elevated acid phosphatase activity mark the macrophage phase, and CD31 and VEGF-R2 outline the expanding microvascularization. In particular, CD45 acts as an integrin, and it is expressed on the surface of myeloid cells. In mammals, CD45 is a pan-leukocyte tyrosine phosphatase, but in *H. verbana*, it preferentially labels macrophage-like cells, highlighting a conserved epitope whose regulation differs in invertebrates.[57,58] Parallel qPCR analyses show a significant increase in two immune factors: *Hv*RNASET2, secreted by granulocytes to attract macrophage-like cells, and *Hm*AIF-1, a proinflammatory cytokine produced by activated phagocytes.[49,59] Their expression aligns with the sequential activation of these immune compartments.

https://doi.org/10.1021/envhealth.5c00268
Environ. Health XXXX, XXX, XXX−XXX

Interestingly, a similar result was also observed for PFMOPrA, whose chronic exposure causes effects residable to PFOA. Again, the full CD11b/CD45/CD31/VEGF-R2 cascade is preserved, confirming the ability of this PFAS congener to sustain the leech inflammatory response over the long term. Remarkably, just as for PFOA, PFMOPrA is also able to induce the production of superoxide dismutase and glutathione-*S*-transferase over time, as confirmed not only by molecular analyses but also by the stimulation of mucus cells that produce these antioxidant enzymes.[34,35] These data are consistent with observations in other freshwater invertebrates such as the cladocera *Daphnia magna* and the rotifer *Brachionus calyciflorus* where long-chain or legacy PFAS (e.g., PFOA and PFOS) affect multiple biological functions regardless of exposure duration.[60,61] Our findings expand the list of PFAS able to drive a complete innate-immune cascade in annelids to include PFMOPrA.

Conversely, weaker results were obtained following HFPO-DA and PFMoBa chronic administration. HFPO-DA, synthesized to replace PFOA with the trademark GenX[20] as well as its five-carbon-atom byproduct PFMoBa, negatively influences the leech immune response by halting the cascade after the granulocyte step. As already observed during the acute treatment,[35] increasing their concentration reduced the number of macrophage-like cells; after two months, a similar result was recorded. Indeed, the acid phosphatase assays show that the number of ACP-positive phagocytes remains extremely low, comparable to the number of controls, and CD45 fluorescence stays at the baseline. This finding is strictly correlated with the absence of blood vessels, which are not visible in morphological analyses or in CD31 and VEGF-R2 staining. The reduced presence of neovessels impairs recruitment of immune precursor cells that normally exploit the circulatory system to reach stimulated areas and differentiate into mature phagocytic cells.[56]

Importantly, the absence of macrophage recruitment should not be interpreted as a sign of reduced toxicity. Rather, it may reflect a form of immunosuppression, in which the activation and differentiation of phagocytic cells are actively impaired. In support of this, *Hm*AIF-1 expression remains low in both HFPO-DA and PFMoBa-treated leeches, suggesting suppression of the phagocyte-derived cytokine response. Thus, failure to progress beyond the granulocyte phase may indicate dysfunctional immune signaling rather than a lower toxic burden. Interestingly, the inhibition of angiogenic processes has also been demonstrated through *in vitro* studies. Comparable inhibition of angiogenesis by PFAS has been reported in vertebrate systems: PFOS reduces tubule formation in HUVECs by interfering with VEGFR-2 signaling,[62] and several PFAS decrease macrophage viability in THP-1-derived cultures.[63] These parallels between annelids and vertebrates highlight the evolutionary conservation of innate-immune and vascular responses, reinforcing the relevance of *H. verbana* as a model for environmental toxicology.

However, although HFPO-DA and PFMoBa inhibit the cell phagocytic arm of inflammation, they still trigger a pronounced CD11b-positive granulocyte influx. The high expression of *Hv*RNASET2, an alarmin released by granulocytes, corroborates this finding.[49,59] Both compounds also stimulate oxidative stress defenses, elevating *SOD*- and *GST*-relative mRNA levels and reactivating mucus cells even after two months of exposure at low concentrations, thus indicating persistent but compartmentalized irritation. Comparable oxidative damage has been reported in mollusks: PFOS induces DNA strand breaks, antioxidant-enzyme imbalance, and apoptosis in the green mussel *Perna viridis* and triggers gill compression, *SOD* upregulation, and metabolic-pathway disruption in the pearl mussel *Hyriopsis cumingii*.[64] Notably, our findings, summarized in Table 3, are consistent with observations in several fish species, where chronic wounds or bacterial infections trigger ROS production by skin mucous cells, subsequently affecting the expression of stress-related enzymes.[65]

Table 3. Summary of Morphological, Inflammatory, and Oxidative Stress Responses Observed in *H. verbana* following PFAS Chronic Exposure[a]

PFAS	angiogenesis (blood vessel density, CD31, VEGF-R2)	granulocyte recruitment (CD11b, *Hv*RNASET2)	macrophage-like cells (CD45, ACP, *Hm*AIF-1)	oxidative stress (mucus cells, *SOD*, *GST*)
PFOA	strong increase	high	high	high
	↑ vessel density	↑ granulocytes	↑ $CD45^+$ cells	↑ mucus cells
	↑ CD31/ VEGF-R2	↑ *Hv*RNASET2	↑ ACP^+ cells	↑ *SOD* and *GST*
			↑ *Hm*AIF-1	
PFMOPrA	strong increase	moderate	high	high
	↑ vessel density	↑ granulocytes	↑ $CD45^+$ cells	↑ mucus cells
	↑ CD31/ VEGF-R2	↑ *Hv*RNASET2	↑ ACP^+ cells	↑ *SOD* and *GST*
			↑ *Hm*AIF-1	
HFPO-DA	no change	high	low	high
		↑ granulocytes	no CD45 or ACP signal	↑ mucus cells
		↑ *Hv*RNASET2	baseline *Hm*AIF-1	↑ *SOD* and *GST*
PFMoBa	no change	moderate	low	high
		↑ granulocytes	no CD45 or ACP signal	↑ mucus cells
		↑ *Hv*RNASET2	baseline *Hm*AIF-1	↑ *SOD* and *GST*
control	baseline	baseline	baseline	baseline

[a]The table compares the effects of each compound on angiogenesis, granulocyte and macrophage-like cell recruitment, and oxidative stress parameters.

To interpret this, PFOA/PFMOPrA vs HFPO-DA/PFMoBa divergence, we consider structure−activity differences, perfluoroalkyl chain length, and ether size/position relative to the acid headgroup and how they shape binding to soluble proteins in the leech circulatory fluid, transporter engagement, and clearance at an equal external dose. Annelids lack serum albumin; oxygen transport relies on giant extracellular hemoglobins (erythrocruorins) and other soluble proteins,[66] so protein binding and the resulting free (unbound) fraction are the relevant determinants of internal exposure. PFMOPrA and PFMoBa share the $-OCF_3$ ether headgroup, but PFMoBa carries one additional CF_2 (C5 vs C4) with the ether slightly farther from the acid, whereas HFPO-DA is a heptafluoropropoxy ($-OC_3F_7$) PFECA rather than a trifluoromethoxy ether. Across PFAS, protein binding generally increases with the perfluoroalkyl length, while ether/branching substitutions tend to reduce binding versus straight-chain PFCAs. Therefore, it is plausible that PFMOPrA exhibits lower binding to soluble circulatory fluid proteins than PFMoBa at 1 nmol L^{-1}, yielding a higher unbound fraction, whereas HFPO-DA shows lower binding and distinct interaction modes than PFOA in mammalian systems, consistent with weaker retention.[67,68] In parallel, transporter studies indicate chain-

https://doi.org/10.1021/envhealth.5c00268
Environ. Health XXXX, XXX, XXX−XXX

length-dependent uptake/retention (e.g., OAT/NTCP/OATP families), with longer-chain PFCAs such as PFOA showing greater transporter-mediated persistence and slower systemic clearance than short-chain PFECAs.[69,70] Taken together, these determinants predict lower effective internal exposure and less sustained signaling for HFPO-DA and (to a lesser extent) PFMoBa than for PFMOPrA and PFOA at 1 nmol L^{-1}, a structure−activity inference that does not exclude a contribution of chain length and that we advance cautiously given the absence of pair-specific binding constants in annelid fluids. While PMPA/PEPA would provide the closest positional match to HFPO-DA, their lack of commercial availability required the use of PFMOPrA/PFMoBa as isomeric substitutes. Therefore, inferences about ether position/size effects are presented as structure−activity hypotheses rather than definitive positional attributions; nevertheless, the reproducible divergence between the C4/C5 methoxy-PFECAs and HFPO-DA at 1 nmol L^{-1} indicates that small changes in the ether architecture can modulate chronic innate-immune and angiogenic outcomes.

It is important to consider other limitations of this work to avoid overinterpretation of the results. First, we tested only a single-dose exposure, which does not allow assessing dose−response relationships or nonlinear effects that are often typical of PFAS. Second, we did not directly measure the actual concentrations of PFAS in the exposure water during the experiment, nor their accumulation in leech tissues. This introduces uncertainty with respect to the effective internal dose experienced by the organisms and requires caution in the interpretation of the results in environmental terms. Third, although *H. verbana* proves to be a sensitive model for innate immunity, angiogenesis, and oxidative stress, it lacks adaptive immune functions and organ-specific physiology, limiting the extent to which long-term or systemic toxicological outcomes can be inferred. It is important to acknowledge the limitations of leeches as a predictive model. While these invertebrates offer a reliable platform to study these mechanisms, they do not possess the complex organ systems proper of vertebrates. These boundaries need to be emphasized to interpret the model correctly and to integrate it with complementary vertebrate data.[37] These constraints highlight the importance of integrating our data with complementary vertebrate studies and dose−response analyses to achieve a comprehensive risk assessment. Nevertheless, acknowledging these limitations strengthens the translational value of the findings, which remain mechanistically consistent with the toxicological outcomes observed across taxa.

5. CONCLUSIONS

Acute and chronic readouts reflect different stages of the same inflammatory process shaped by PFAS chemistry and exposure time. Short-term end points alone can therefore mischaracterize eventual hazard if longer-term dynamics are not considered. At a policy-relevant low dose (1 nmol L^{-1}) over two months, the initial defensive wave either persists and matures into the full CD11b/CD45/CD31 cascade with elevated oxidative stress and immune transcripts (PFOA and PFMOPrA) or stalls after the granulocyte stage (HFPO-DA and PFMoBa), yielding divergent physiological outcomes. These patterns indicate that structure−activity determinants, including the ether size/position and perfluoroalkyl length, extend beyond the nominal chain length in shaping chronic responses at 1 nmol L^{-1}. Of note, we do not exclude a contribution of chain length. Together, the results argue for multitemporal, low-dose designs as standard practice in PFAS hazard assessment.

AUTHOR INFORMATION

Corresponding Author

Annalisa Grimaldi − *Department of Biotechnology and Life Sciences, University of Insubria, Varese 21100, Italy*; Phone: +39 0332 421325; Email: annalisa.grimaldi@uninsubria.it

Authors

Nicolò Baranzini − *Department of Biotechnology and Life Sciences, University of Insubria, Varese 21100, Italy*; orcid.org/0000-0001-6996-4797

Antonio Calisi − *Department of Science and Technological Innovation, University of Eastern Piedmont, Alessandria 15121, Italy*

Gaia Marcolli − *Department of Biotechnology and Life Sciences, University of Insubria, Varese 21100, Italy*

Camilla Bon − *Department of Biotechnology and Life Sciences, University of Insubria, Varese 21100, Italy*

Davide Rotondo − *Department of Science and Technological Innovation, University of Eastern Piedmont, Alessandria 15121, Italy*

Davide Gualandris − *Department of Science and Technological Innovation, University of Eastern Piedmont, Alessandria 15121, Italy*

Laura Pulze − *Department of Biotechnology and Life Sciences, University of Insubria, Varese 21100, Italy*

Francesco Dondero − *Department of Science and Technological Innovation, University of Eastern Piedmont, Alessandria 15121, Italy*

Complete contact information is available at: https://pubs.acs.org/10.1021/envhealth.5c00268

Author Contributions

‡N.B. and A.C. equally contributed to the work. N.B.: Investigation, data curation, formal analysis, writing of the original draft, visualization, and validation. A.C.: Investigation, data curation, formal analysis, writing of the original draft, visualization, and validation. G.M.: Methodologies, data curation, and review and editing. C.B.: Methodologies, data curation, and review and editing. D.G.: Data curation and review and editing. D.R.: Data curation and review and editing. L.P.: Validation, data curation, and review and editing. A.G.: Conceptualization, project administration, writing of the original draft, and supervision. F.D.: Conceptualization, funding, materials, project administration, writing of the original draft, and supervision.

Funding

This project has received funding from the European Union's Horizon 2020 research and innovation program under grant agreement no. 101037509 (SCENARIOS project) and from Insubria Academic Research Funds (FAR) 2024 to N.B. and A.G.

Notes

G.M. and C.B. are PhD students of Life Sciences and Biotechnology Course at the University of Insubria.
The authors declare no competing financial interest.

ABBREVIATIONS

ACP, acid phosphatase assay; DAPI, 4,6-diamidino-2-phenylindole; GAPDH, D-glyceraldehyde-3-phosphate dehydrogenase; *GST*, glutathione-*S*-transferase; HFPO-DA, hexafluoropro-

https://doi.org/10.1021/envhealth.5c00268
Environ. Health XXXX, XXX, XXX−XXX

pylene-oxide dimer acid; *Hm*AIF-1, *Hirudo medicinalis* allograph inflammatory factor-1; *Hv*RNASET2, *Hirudo verbana* RNASET2; PAS, periodic acid−Schiff; PFAS, per- and polyfluoroalkyl substances; PFMOPrA, perfluoro-3-methoxypropanoic acid; PFMoBa, perfluoro(4-methoxybutanoic) acid; PFOS, perfluorooctanesulfonic acid; PFOA, perfluorooctanoic acid; *SOD*, superoxide dismutase

REFERENCES

(1) Göckener, B.; Weber, T.; Rüdel, H.; Bücking, M.; Kolossa-Gehring, M. Human Biomonitoring of Per- and Polyfluoroalkyl Substances in German Blood Plasma Samples from 1982 to 2019. *Environ. Int.* **2020**, *145*, No. 106123.

(2) Kaiser, A. M.; Forsthuber, M.; Widhalm, R.; Granitzer, S.; Weiss, S.; Zeisler, H.; Foessleitner, P.; Salzer, H.; Grasl-Kraupp, B.; Moshammer, H.; Hartmann, C.; Uhl, M.; Gundacker, C. Prenatal Exposure to Per- and Polyfluoroalkyl Substances and Pregnancy Outcome in Austria. *Ecotoxicol Environ. Saf* **2023**, *259*, No. 115006.

(3) Worley, R. R.; Moore, S. M. A.; Tierney, B. C.; Ye, X.; Calafat, A. M.; Campbell, S.; Woudneh, M. B.; Fisher, J. Per- and Polyfluoroalkyl Substances in Human Serum and Urine Samples from a Residentially Exposed Community. *Environ. Int.* **2017**, *106*, 135−143.

(4) *Registry of restriction intentions until outcome - ECHA*https://echa.europa.eu/registry-of-restriction-intentions/-/dislist/details/0b0236e18663449b (accessed 2025−08−04).

(5) McCarthy, C.; Kappleman, W.; DiGuiseppi, W. Ecological Considerations of Per- and Polyfluoroalkyl Substances (PFAS). *Curr. Pollut Rep* **2017**, *3* (4), 289−301.

(6) Sinclair, G. M.; Long, S. M.; Jones, O. A. H. What Are the Effects of PFAS Exposure at Environmentally Relevant Concentrations? *Chemosphere* **2020**, *258*, No. 127340.

(7) Herzke, D.; Huber, S.; Bervoets, L.; D'Hollander, W.; Hajslova, J.; Pulkrabova, J.; Brambilla, G.; De Filippis, S. P.; Klenow, S.; Heinemeyer, G.; de Voogt, P. Perfluorinated Alkylated Substances in Vegetables Collected in Four European Countries; Occurrence and Human Exposure Estimations. *Environ. Sci. Pollut. Res.* **2013**, *20* (11), 7930−7939.

(8) Longpré, D.; Lorusso, L.; Levicki, C.; Carrier, R.; Cureton, P. PFOS, PFOA, LC-PFCAS, and Certain Other PFAS: A Focus on Canadian Guidelines and Guidance for Contaminated Sites Management. *Environ. Technol. Innov* **2020**, *18*, No. 100752.

(9) Furlow, B. US EPA Sets Historic New Restrictions on Toxic PFAS in Drinking Water. *Lancet Oncol* **2024**, *25* (5), No. e181.

(10) Mantripragada, S.; Obare, S. O.; Zhang, L. Addressing Short-Chain PFAS Contamination in Water with Nanofibrous Adsorbent/Filter Material from Electrospinning. *Acc. Chem. Res.* **2023**, *56* (11), 1271−1278.

(11) Pietropoli, E.; Bardhi, A.; Simonato, V.; Zanella, M.; Iori, S.; Barbarossa, A.; Giantin, M.; Dacasto, M.; De Liguoro, M.; Pauletto, M. Comparative Toxicity Assessment of Alternative versus Legacy PFAS: Implications for Two Primary Trophic Levels in Freshwater Ecosystems. *J. Hazard Mater.* **2024**, *477*, No. 135269.

(12) *FINAL FRESHWATER AQUATIC LIFE AMBIENT WATER QUALITY CRITERIA AND ACUTE SALTWATER AQUATIC LIFE BENCHMARK for PERFLUOROOCTANOIC ACID (PFOA)***2024**.

(13) Epa, U.; of Ground Water, O.; Water, D.*Final PFAS National Primary Drinking Water Regulation*; United States Environmental Protection Agency, **2024**

(14) Hill, P. J.; Taylor, M.; Goswami, P.; Blackburn, R. S. Substitution of PFAS Chemistry in Outdoor Apparel and the Impact on Repellency Performance. *Chemosphere* **2017**, *181*, 500−507.

(15) Jane L Espartero, L.; Yamada, M.; Ford, J.; Owens, G.; Prow, T.; Juhasz, A. Health-Related Toxicity of Emerging per- and Polyfluoroalkyl Substances: Comparison to Legacy PFOS and PFOA. *Environ. Res.* **2022**, *212*, No. 113431.

(16) Mahoney, H.; Xie, Y.; Brinkmann, M.; Giesy, J. P. Next Generation Per- and Poly-Fluoroalkyl Substances: Status and Trends, Aquatic Toxicity, and Risk Assessment. *Eco-Environment & Health* **2022**, *1* (2), 117−131.

(17) Peschka, M.; Fichtner, N.; Hierse, W.; Kirsch, P.; Montenegro, E.; Seidel, M.; Wilken, R. D.; Knepper, T. P. Synthesis and Analytical Follow-up of the Mineralization of a New Fluorosurfactant Prototype. *Chemosphere* **2008**, *72* (10), 1534−1540.

(18) Podder, A.; Sadmani, A. H. M. A.; Reinhart, D.; Chang, N. B.; Goel, R. Per and Poly-Fluoroalkyl Substances (PFAS) as a Contaminant of Emerging Concern in Surface Water: A Transboundary Review of Their Occurrences and Toxicity Effects. *J. Hazard Mater.* **2021**, *419* (March), No. 126361.

(19) Panieri, E.; Baralic, K.; Djukic-Cosic, D.; Buha Djordjevic, A.; Saso, L. PFAS Molecules: A Major Concern for the Human Health and the Environment. *Toxics* **2022**, *10* (2), 44.

(20) Brase, R. A.; Mullin, E. J.; Spink, D. C. Legacy and Emerging Per- and Polyfluoroalkyl Substances: Analytical Techniques, Environmental Fate, and Health Effects. *Int. J. Mol. Sci.* **2021**, *22* (3), 995.

(21) Li, Y.; Yao, J.; Pan, Y.; Dai, J.; Tang, J. Trophic Behaviors of PFOA and Its Alternatives Perfluoroalkyl Ether Carboxylic Acids (PFECAs) in a Coastal Food Web. *J. Hazard Mater.* **2023**, *452* (April), No. 131353.

(22) Nayak, S.; Sahoo, G.; Das, I. I.; Mohanty, A. K.; Kumar, R.; Sahoo, L.; Sundaray, J. K. Poly- and Perfluoroalkyl Substances (PFAS): Do They Matter to Aquatic Ecosystems? *Toxics* **2023**, *11* (6), 543.

(23) Sima, M. W.; Jaffé, P. R. A Critical Review of Modeling Poly- and Perfluoroalkyl Substances (PFAS) in the Soil-Water Environment. *Sci. Total Environ.* **2021**, *757*, No. 143793.

(24) Mahinroosta, R.; Senevirathna, L. A Review of the Emerging Treatment Technologies for PFAS Contaminated Soils. *J. Environ. Manage* **2020**, *255* (December 2019), No. 109896.

(25) Crone, B. C.; Speth, T. F.; Wahman, D. G.; Smith, S. J.; Abulikemu, G.; Kleiner, E. J.; Pressman, J. G. Source Water and Their Treatment in Drinking Water. *Environ. Sci. Technol.* **2019**, *49* (24), 2359−2396.

(26) Kurwadkar, S.; Dane, J.; Kanel, S. R.; Nadagouda, M. N.; Cawdrey, R. W.; Ambade, B.; Struckhoff, G. C.; Wilkin, R. Per- and Polyfluoroalkyl Substances in Water and Wastewater: A Critical Review of Their Global Occurrence and Distribution. *Sci. Total Environ.* **2022**, *809*, No. 151003.

(27) Sadia, M.; Kunz, M.; ter Laak, T.; De Jonge, M.; Schriks, M.; van Wezel, A. P. Forever Legacies? Profiling Historical PFAS Contamination and Current Influence on Groundwater Used for Drinking Water. *Sci. Total Environ.* **2023**, *890* (March), No. 164420.

(28) Ehrlich, V.; Bil, W.; Vandebriel, R.; Granum, B.; Luijten, M.; Lindeman, B.; Grandjean, P.; Kaiser, A. M.; Hauzenberger, I.; Hartmann, C.; Gundacker, C.; Uhl, M. Consideration of Pathways for Immunotoxicity of Per- and Polyfluoroalkyl Substances (PFAS). *Environ. Health* **2023**, *22* (1), 1−47.

(29) *Volume 135: Perfluorooctanoic acid (PFOA) and perfluorooctanesulfonic acid (PFOS) − IARC Monographs on the Identification of Carcinogenic Hazards to Humans*. https://monographs.iarc.who.int/news-events/volume-135-perfluorooctanoic-acid-pfoa-and-perfluorooctanesulfonic-acid-pfos/ (accessed 2025−08−04).

(30) Sawyer, L.; Roy, T.Leech Behavior, in *Neurobiology of the Leech*; Cold Spring Harbor, 1981.

(31) de Eguileor, M.; Grimaldi, A.; Tettamanti, G.; Ferrarese, R.; Congiu, T.; Protasoni, M.; Perletti, G.; Valvassori, R.; Lanzavecchia, G. Hirudo Medicinalis: A New Model for Testing Activators and Inhibitors of Angiogenesis. *Angiogenesis* **2001**, *4* (4), 299−312.

(32) Macagno, E. R.; Gaasterland, T.; Edsall, L.; Bafna, V.; Soares, M. B.; Scheetz, T.; Casavant, T.; Da Silva, C.; Wincker, P.; Tasiemski, A.; Salzet, M. Construction of a Medicinal Leech Transcriptome Database and Its Application to the Identification of Leech Homologs of Neural and Innate Immune Genes. *BMC Genomics* **2010**, *11* (1), 407.

(33) Girardello, R.; Tasselli, S.; Baranzini, N.; Valvassori, R.; de Eguileor, M.; Grimaldi, A.; LI, M. Effects of Carbon Nanotube Environmental Dispersion on an Aquatic Invertebrate Hirudo Medicinalis. *PLoS One* **2015**, *10* (12), e0144361−16.

https://doi.org/10.1021/envhealth.5c00268
Environ. Health XXXX, XXX, XXX−XXX

(34) Baranzini, N.; Pulze, L.; Bon, C.; Izzo, L.; Pragliola, S.; Venditto, V.; Grimaldi, A. Hirudo Verbana as a Freshwater Invertebrate Model to Assess the Effects of Polypropylene Micro and Nanoplastics Dispersion in Freshwater. *Fish Shellfish Immunol* **2022**, *127* (May), 492−507.
(35) Calisi, A.; Baranzini, N.; Marcolli, G.; Bon, C.; Rotondo, D.; Gualandris, D.; Pulze, L.; Grimaldi, A.; Dondero, F. Evaluation of Per- and Polyfluoroalkyl Substances (PFAS) Toxic Effects on the Acute Inflammatory Response in the Medicinal Leech Hirudo Verbana. *Chemosphere* **2024**, *366* (October), No. 143519.
(36) Girardello, R.; Baranzini, N.; Tettamanti, G.; de Eguileor, M.; Grimaldi, A. Cellular Responses Induced by Multi-Walled Carbon Nanotubes: In Vivo and in Vitro Studies on the Medicinal Leech Macrophages. *Sci. Rep* **2017**, *7* (1), 1−12.
(37) Bodó, K.; Baranzini, N.; Girardello, R.; Kokhanyuk, B.; Németh, P.; Hayashi, Y.; Grimaldi, A.; Engelmann, P. Nanomaterials and Annelid Immunity: A Comparative Survey to Reveal the Common Stress and Defense Responses of Two Sentinel Species to Nanomaterials in the Environment. *Biology* **2020**, *9* (10), 307−322.
(38) Rosner, A.; Ballarin, L.; Barnay-Verdier, S.; Borisenko, I.; Drago, L.; Drobne, D.; Concetta Eliso, M.; Harbuzov, Z.; Grimaldi, A.; Guy-Haim, T.; Karahan, A.; Lynch, I.; Giulia Lionetto, M.; Martinez, P.; Mehennaoui, K.; Oruc Ozcan, E.; Pinsino, A.; Paz, G.; Rinkevich, B.; Spagnuolo, A.; Sugni, M.; Cambier, S. A Broad-Taxa Approach as an Important Concept in Ecotoxicological Studies and Pollution Monitoring. *Biol. Rev.* **2024**, *99* (1), 131−176.
(39) Eguileor, M. d.; Grimaldi, A.; Tettamanti, G.; Valvassori, R.; Cooper, E. L.; Lanzavecchia, G. Different Types of Response to Foreign Antigens by Leech Leukocytes. *Tissue Cell* **2000**, *32* (1), 40−48.
(40) Schorn, T.; Drago, F.; Tettamanti, G.; Valvassori, R.; de Eguileor, M.; Vizioli, J.; Grimaldi, A. Homolog of Allograft Inflammatory Factor-1 Induces Macrophage Migration during Innate Immune Response in Leech. *Cell Tissue Res.* **2015**, *359*, 853−864.
(41) Tettamanti, G.; Grimaldi, A.; Valvassori, R.; Rinaldi, L.; de Eguileor, M. Vascular Endothelial Growth Factor Is Involved in Neoangiogenesis in Hirudo Medicinalis (Annelida, Hirudinea). *Cytokine* **2003**, *22* (6), 168−179.
(42) Sun, M.; Arevalo, E.; Strynar, M.; Lindstrom, A.; Richardson, M.; Kearns, B.; Pickett, A.; Smith, C.; Knappe, D. R. U. Legacy and Emerging Perfluoroalkyl Substances Are Important Drinking Water Contaminants in the Cape Fear River Watershed of North Carolina. *Environ. Sci. Technol. Lett.* **2016**, *3* (12), 415−419.
(43) Hopkins, Z. R.; Sun, M.; DeWitt, J. C.; Knappe, D. R. U. Recently Detected Drinking Water Contaminants: GenX and Other Per- and Polyfluoroalkyl Ether Acids. *J. Am. Water Works Assoc* **2018**, *110* (7), 13−28.
(44) *ASSESSMENT OF THE CHEMICAL AND SPATIAL DISTRIBUTION OF PFAS IN THE CAPE FEAR RIVER*. **2018**.
(45) Tang, A.; Zhang, X.; Li, R.; Tu, W.; Guo, H.; Zhang, Y.; Li, Z.; Liu, Y.; Mai, B. Spatiotemporal Distribution, Partitioning Behavior and Flux of per- and Polyfluoroalkyl Substances in Surface Water and Sediment from Poyang Lake. *China. Chemosphere* **2022**, *295*, No. 133855.
(46) Hong, Y.; Ding, Q.; Yang, T.; Li, X.; Song, N.; Zhang, J. Per- and Polyfluoroalkyl Substances (PFAS) in Drinking Water Systems in the Lower Yangtze River: Source, Fate, and Health Risk Assessment. *Environ. Geochem. Health* **2025**, *47* (6), 1−16.
(47) Li, Y.; Yao, J.; Zhang, J.; Pan, Y.; Dai, J.; Ji, C.; Tang, J. First Report on the Bioaccumulation and Trophic Transfer of Perfluoroalkyl Ether Carboxylic Acids in Estuarine Food Web. *Environ. Sci. Technol.* **2022**, *56* (10), 6046−6055.
(48) Baranzini, N.; Pulze, L.; Acquati, F.; Grimaldi, A. Hirudo Verbana as an Alternative Model to Dissect the Relationship between Innate Immunity and Regeneration. *Invertebrate Survival J.* **2020**, *17* (1), 90−98.
(49) Baranzini, N.; Monti, L.; Vanotti, M.; Orlandi, V. T.; Bolognese, F.; Scaldaferri, D.; Girardello, R.; Tettamanti, G.; de Eguileor, M.; Vizioli, J.; Taramelli, R.; Acquati, F.; Grimaldi, A. AIF-1 and RNASET2 Play Complementary Roles in the Innate Immune Response of Medicinal Leech. *J. Innate Immun* **2019**, *11* (2), 150−167.
(50) Schorn, T.; Drago, F.; de Eguileor, M.; Valvassori, R.; Vizioli, J.; Tettamanti, G.; Grimaldi, A. The Allograft Inflammatory Factor-1 (AIF-1) Homologous in Hirudo Medicinalis (Medicinal Leech) Is Involved in Immune Response during Wound Healing and Graft Rejection Processes. *Invertebrate Survival J.* **2015**, *12*, 129−141.
(51) Parolini, M.; De Felice, B.; Rusconi, M.; Morganti, M.; Polesello, S.; Valsecchi, S. A Review of the Bioaccumulation and Adverse Effects of PFAS in Free-Living Organisms from Contaminated Sites Nearby Fluorochemical Production Plants. *Water Emerging Contaminants & Nanoplastics* **2022**, *1* (4), 18.
(52) Zahm, S.; Bonde, J. P.; Chiu, W. A.; Hoppin, J.; Kanno, J.; Abdallah, M.; Blystone, C. R.; Calkins, M. M.; Dong, G. H.; Dorman, D. C.; Fry, R.; Guo, H.; Haug, L. S.; Hofmann, J. N.; Iwasaki, M.; Machala, M.; Mancini, F. R.; Maria-Engler, S. S.; Møller, P.; Ng, J. C.; Pallardy, M.; Post, G. B.; Salihovic, S.; Schlezinger, J.; Soshilov, A.; Steenland, K.; Steffensen, I. L.; Tryndyak, V.; White, A.; Woskie, S.; Fletcher, T.; Ahmadi, A.; Ahmadi, N.; Benbrahim-Tallaa, L.; Bijoux, W.; Chittiboyina, S.; de Conti, A.; Facchin, C.; Madia, F.; Mattock, H.; Merdas, M.; Pasqual, E.; Suonio, E.; Viegas, S.; Zupunski, L.; Wedekind, R.; Schubauer-Berigan, M. K. Carcinogenicity of Perfluorooctanoic Acid and Perfluorooctanesulfonic Acid. *Lancet Oncol.* **2024**, *25* (1), 16−17.
(53) Li, K.; Gao, P.; Xiang, P.; Zhang, X.; Cui, X.; Ma, L. Q. Molecular Mechanisms of PFOA-Induced Toxicity in Animals and Humans: Implications for Health Risks. *Environ. Int.* **2017**, *99*, 43−54.
(54) Lagostena, L.; Rotondo, D.; Gualandris, D.; Calisi, A.; Lorusso, C.; Magnelli, V.; Dondero, F. Impact of Legacy Perfluorooctane Sulfonate (PFOS) and Perfluorooctanoate (PFOA) on GABA Receptor-Mediated Currents in Neuron-Like Neuroblastoma Cells: Insights into Neurotoxic Mechanisms and Health Implications. *J. Xenobiotics* **2024**, *14* (4), 1771−1783.
(55) Grimaldi, A.; Tettamanti, G.; de Eguileor, M. Annelida: Hirudinea (Leeches): Heterogeneity in Leech Immune Responses. *Advances in Comparative Immunology* **2018**, 173−191.
(56) Grimaldi, A. Origin and Fate of Hematopoietic Stem Precursor Cells in the Leech Hirudo Medicinalis. *Invertebrate Survival J.* **2016**, *13* (1), 257−268.
(57) Roach, T.; Slater, S.; Koval, M.; White, L.; McFarland, E. C.; Okumura, M.; Thomas, M.; Brown, E. CD45 Regulates Src Family Member Kinase Activity Associated with Macrophage Integrin-Mediated Adhesion. *Curr. Biol.* **1997**, *7* (6), 408−417.
(58) St-Pierre, J.; Ostergaard, H. L. A Role for the Protein Tyrosine Phosphatase CD45 in Macrophage Adhesion through the Regulation of Paxillin Degradation. *PLoS One* **2013**, *8* (7), No. e71531.
(59) Baranzini, N.; De Vito, A.; Orlandi, V. T.; Reguzzoni, M.; Monti, L.; de Eguileor, M.; Rosini, E.; Pollegioni, L.; Tettamanti, G.; Acquati, F.; Grimaldi, A. Antimicrobial Role of RNASET2 Protein During Innate Immune Response in the Medicinal Leech Hirudo Verbana. *Front Immunol* **2020**, *11* (March), 1−18.
(60) Zhang, L.; Niu, J.; Li, Y.; Wang, Y.; Sun, D. Evaluating the Sub-Lethal Toxicity of PFOS and PFOA Using Rotifer Brachionus Calyciflorus. *Environ. Pollut.* **2013**, *180*, 34−40.
(61) Barmentlo, S. H.; Stel, J. M.; Van Doorn, M.; Eschauzier, C.; De Voogt, P.; Kraak, M. H. S. Acute and Chronic Toxicity of Short Chained Perfluoroalkyl Substances to Daphnia Magna. *Environ. Pollut.* **2015**, *198*, 47−53.
(62) Forsthuber, M.; Widhalm, R.; Granitzer, S.; Kaiser, A. M.; Moshammer, H.; Hengstschläger, M.; Dolznig, H.; Gundacker, C. Perfluorooctane Sulfonic Acid (PFOS) Inhibits Vessel Formation in a Human 3D Co-Culture Angiogenesis Model (NCFs/HUVECs). *Environ. Pollut.* **2022**, *293* (June), No. 118543.
(63) Amstutz, V. H.; Sijm, D. T. H. M.; Vrolijk, M. F. Perfluoroalkyl Substances and Immunotoxicity: An in Vitro Structure-Activity Relationship Study in THP-1-Derived Monocytes and Macrophages. *Chemosphere* **2024**, *364* (August), No. 143075.
(64) Ma, T.; Wu, P.; Wang, L.; Li, Q.; Li, X.; Luo, Y. Toxicity of Per- and Polyfluoroalkyl Substances to Aquatic Vertebrates. *Front Environ. Sci.* **2023**, *11*, 1101100.

https://doi.org/10.1021/envhealth.5c00268
Environ. Health XXXX, XXX, XXX−XXX

(65) Cordero, H.; Brinchmann, M. F.; Cuesta, A.; Esteban, M. A. Chronic Wounds Alter the Proteome Profile in Skin Mucus of Farmed Gilthead Seabream. *BMC Genomics* **2017**, *18* (1), 939.
(66) Royer, W. E.; Strand, K.; Van Heel, M.; Hendrickson, W. A. Structural Hierarchy in Erythrocruorin, the Giant Respiratory Assemblage of Annelids. *Proc. Natl. Acad. Sci. U. S. A.* **2000**, *97* (13), 7107−7111.
(67) Jackson, T. W.; Scheibly, C. M.; Polera, M. E.; Belcher, S. M. Rapid Characterization of Human Serum Albumin Binding for Per- and Polyfluoroalkyl Substances Using Differential Scanning Fluorimetry. *Environ. Sci. Technol.* **2021**, *55* (18), 12291−12301.
(68) Starnes, H. M.; Jackson, T. W.; Rock, K. D.; Belcher, S. M. Quantitative Cross-Species Comparison of Serum Albumin Binding of per- and Polyfluoroalkyl Substances from Five Structural Classes. *Toxicol. Sci.* **2024**, *199* (1), 132−149.
(69) Vujic, E.; Ferguson, S. S.; Brouwer, K. L. R. Effects of PFAS on Human Liver Transporters: Implications for Health Outcomes. *Toxicol. Sci.* **2024**, *200* (2), 213−227.
(70) Ryu, S.; Yamaguchi, E.; Sadegh Modaresi, S. M.; Agudelo, J.; Costales, C.; West, M. A.; Fischer, F.; Slitt, A. L. Evaluation of 14 PFAS for Permeability and Organic Anion Transporter Interactions: Implications for Renal Clearance in Humans. *Chemosphere* **2024**, *361*, No. 142390.

https://doi.org/10.1021/envhealth.5c00268
Environ. Health XXXX, XXX, XXX−XXX